Physica Medica 68 (2019) 61–68

Contents lists available at ScienceDirect

Physica Medica

journal homepage: www.elsevier.com/locate/ejmp

Original paper

Dose optimisation in paediatric radiography – Using regression models to investigate the relative impact of acquisition factors on image quality and radiation dose

Ali Mohammed Ali[a,*], Peter Hogg[b], Andrew England[b]

[a] College of Health and Medical Technology, University of Al Zahraa for Women, Karbala, Iraq
[b] School of Health & Society, University of Salford, Salford M6 6PU, United Kingdom

ARTICLE INFO

Keywords:
Pelvis radiography
Paediatric dose reduction
Regression analysis
Exposure factor impact
Digital radiography

ABSTRACT

Objective: To investigate the optimum pelvis X-ray acquisition factors for a 10-year-old child. Secondly, to evaluate the impact of each acquisition factor on image quality (IQ) and radiation dose.
Method: Images were acquired using a pelvis phantom and a range of acquisition parameters; e.g. tube potential, additional filtration and source-to-image distance (SID). Automatic exposure control (AEC) was used with two orientations (head towards/away from two outer chambers) and three different chamber selections. Visual IQ was evaluated using relative and absolute-VGA methods. Radiation doses were measured by placing a dosimeter on the anterior surface of the phantom. Regression analysis was used to determine optimum parameters.
Results: The optimised technique (178.8 μGy), with diagnostic IQ, was with 89kVp, 130 cm SID and with 1 mm Al + 0.1 mm Cu filtration. This technique was with the head towards the two outer AEC chambers. Regression analysis showed that SID had the lowest impact on IQ (β = 0.002 95% CI −0.001 to 0.005) and dose (β = −0.96 95% CI −0.40 to −1.53). The impact of filtration on dose (β = −76.24 95% CI −86.76 to −85.72) was higher than tube potential (β = −13.44 95% CI −14.34 to −12.53). The following impact ratios were higher on IQ than radiation dose: filtration/kVp; 11.28 times, filtration/SID; 7.01 times and kVp/SID; 0.62 times.
Conclusion: Optimised parameters were identified as 89 kVp, 130 cm SID and with 1 mm Al + 0.1 mm Cu additional filtration. Regression analysis demonstrated that filtration and tube potential had the greatest effect on radiation dose and IQ, respectively.

1. Introduction

The widespread move to digital radiography (DR) has brought additional challenges to balancing image quality (IQ) with radiation dose. The energy responses of digital detectors are significantly different from film-screen, and DR offers greater flexibility in utilising low levels of radiation and when processing an image [1]. Unlike film-screen, if the radiation dose to the image detector is increased, the IQ can stay diagnostically acceptable or even improve [2]. On the other hand, if the dose to the detector is decreased, the images may start to appear noisy [2]. Thus, there is a need for the standardisation of DR protocols and exposure parameters to remain committed toward the ALARA principle [3].

Researchers have used different approaches for dose optimisation. Some [4,5] collected X-ray images from hospitals to perform dose optimisation. However, such studies include limitations through variations in weight and age ranges, which raises questions regarding the validity of the their results [6]. The limited variations in the exposure factors examined (i.e. kVp, mAs, SID and filtration ranges) add another limitation to their measured outcomes. Others have sought to represent a 5 year-old child's hip using animal specimens, such as a lamb's femur [7]. However, the size and anatomical shape of these vary considerably when compared to a human. Others have undertaken optimisation studies using test objects, such as the CDRAD phantom [8,9]. These phantoms are limited due to the lack of anatomical noise in the images [10]. Other researchers have attempted to optimise acquisition parameters in paediatric pelvic imaging using dosimetry phantoms (such as the ATOM phantom) [11–13]. Such phantoms can misrepresent the density of bone tissue due to their use of an averaged density for both the cortical and trabecular bone [14], and thus the contrast of all bony structures may be underestimated. There are also limitations when comparing patient-specific anatomical shapes to those

* Corresponding author.
E-mail addresses: a.h.m.a.mohammedali@edu.salford.ac.uk (A. Mohammed Ali), P.Hogg@salford.ac.uk (P. Hogg), A.England@salford.ac.uk (A. England).

https://doi.org/10.1016/j.ejmp.2019.10.034
Received 30 January 2019; Received in revised form 20 October 2019; Accepted 21 October 2019
Available online 18 November 2019

(a) (b)

Fig. 1. (1: a and b): (a) shows the setup for acquiring X-ray images; (b) shows the setup for measuring radiation dose.

used in anthropomorphic phantoms.

All the aforementioned studies have considered only one or two exposure factors, neglecting the combined effects of the other exposure factors. Also, these studies did not conduct a full factorial design including the possible effects from all exposure factors, adding another limitation to validity of their outcomes [15,16]. Several recent studies have demonstrated the need for dose optimisation in DR [3,17,18]. Exposure factors, such as tube potential (kVp), tube current-time (mAs), source to image distance (SID) and added filtration have well-defined effects on radiation dose [19], however their effect on IQ within paediatric pelvis radiography is not established. Moreover, interactions with other factors have not been fully investigated and such explorations should help to determine which exposure factor or factors have the greater effect on radiation dose than on IQ, or vice versa. Thus, radiographers will be able to choose different exposure factors to achieve the maximum dose reduction with the smallest effect on IQ. Thus, this study investigates the dose-optimised exposure factors using systematic variations (full factorial design) of radiographic exposure factors with an anthropomorphic pelvis phantom representing a 10-year-old child. This study also compares the effect of each exposure factor on IQ and radiation dose.

2. Material and methods

2.1. Data acquisition

A series of X-ray exposures were carried out using a range of acquisition factors. The factors were based on the opinions of several experienced paediatric diagnostic radiographers and were proposed for the production of an acceptable image quality at low dose when imaging the pelvis of a ten year old. Also, the proposed exposure factors were in agreement with the European Guidelines for Paediatric Radiography [20]. Tube potentials ranged from 59 to 89 kVp, in 3 kVp increments. The applied filtration levels were: zero filtration, 2 mm Al and 1 mm Al + 0.1 mm Cu. The SID, measured from the X-ray tube to the image detector, included 100, 115, 130 and 140 cm. 140 cm was set as the maximum because the distance between the X-ray tube and the table mounted detector could not extend beyond this. All acquisitions used automatic exposure control (AEC) and a parallel oscillating anti-scatter secondary radiation grid. The exposure factor combinations were repeated for two different orientations: head away (HA) from the two outer AEC chambers and head towards (HT) the two outer AEC chambers. For each orientation, three combinations of ionisation chambers were selected: all three chambers, the two outer chambers and the middle chamber. The total number of images acquired was 792.

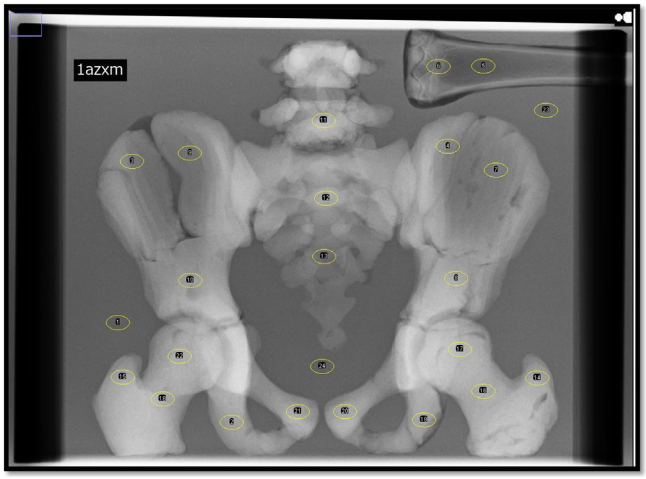

Fig. 2. Locations of the ROI measurements on the 10-year-old phantom image using the ImageJ software.

The X-ray tube was a Wolverson Arcoma Arco Ceil general radiography system (Arcoma, Annavägen, Sweden), with a high frequency generator and a VARIAN 130 HS X-ray tube. This unit had total filtration of 3 mm Al (i.e. inherent 0.5 and added 2.5 mm). A fixed anti-scatter grid (10:1 ratio, 40 line/cm frequency) was used for all acquisitions as this grid is commonly used in clinical settings [21], and has been recommended in the literature [20] and from discussions with experienced radiographers.

The images were generated using a bespoke anthropomorphic phantom (Fig. 3). The phantom was 15 cm thick and contained radiological tissue substitutes for bone (Plaster of Paris) and soft-tissue (PMMA), which simulated a 10-year-old child's pelvis. Phantom validation utilised computed tomography (CT) data from a 10-year-old child, using a method described in literature [22]. There was a number of radiolucencies present in the phantom X-ray images, which resulted from a failure to completely fill the PMMA voids with Plaster of Paris. Such radiolucencies are an accepted part of the phantom manufacturing process and have been reported previously in the literature [22]. However, for the method in this study, the visual and physical IQ analyses avoided the radiolucent areas by ensuring the ROIs were placed outside of them and observer evaluations were conducted away from them too. The image detector was a Konica Minolta Aero direct digital radiography (DR) system (model CS-7; Aero DR System, Konica Minolta Medical Imaging, USA INC, Wayne, NJ).

The images for each exposure combination were generated by placing the phantom on the X-ray table – see Fig. 1a. Radiation doses were represented by incident air kerma (IAK), for each exposure factor combination. These were measured at the surface of the phantom (see Fig. 1b) using a solid-state dosimeter (Raysafe X2, Unfors Raysafe AB, Billdal, Sweden) that was placed in the centre of the collimation.

Equipment quality assurance testing was performed prior to image acquisition and included an assessment of voltage accuracy, exposure time, field size collimation and AEC sensitivity. The AEC sensitivity adjustments were kept at the manufacturer's default settings. In addition, the consistency of the solid-state dosimeter was verified. Testing followed IPEM 91 guidance [23], and all results were found to be within the expected manufacturer tolerances.

2.2. Image quality and radiation dose assessment

IQ was evaluated perceptually using two methods – relative Visual Grading Analysis (VGA) and absolute (binary: yes/no). For the relative-VGA [24], the images from the paediatric pelvis phantoms were displayed randomly in DICOM format using dedicated software [25]. A 3-point Likert scale was applied to assess the visual IQ. An observer (lead researcher in this study) assessed the image sharpness and noise of specific anatomical areas (the femoral heads, femoral epiphysis, pubic bones, ischium, sacro-iliac joints, femoral necks, sacrum, L5 vertebral body and iliac crests, in addition to animal bone (lamb that included both cortical and trabecular bone)), by use of an IQ score (worse (2), equal to (3), or better than (4)), against that of a 'reference image' of median IQ. Images were displayed using two monitors: the left one displayed the reference image and the right one displayed the range of experimental images in a random and anonymised fashion. The monitors were 5 mega-pixel monochrome liquid crystal (LCD), manufactured by DOME E5 (NDSsi, Santa Rosa, Ca) and calibrated to the DICOM grey-scale standard function. The ambient room lighting was dimmed to simulate clinical imaging conditions, at approximately 30 Lux [26]. A total of 19 criteria were included in the relative VGA study. These criteria had previously been developed and validated by Mraity et al. (2016), see Table 4 in the appendix [27].

The reference image was chosen using physical IQ (SNR) and visual evaluation. First, the SNR was measured using ImageJ software version 1.49 (NIH, Maryland, US) from the regions of interest (ROI) located in the same bony anatomy used in the relative-VGA assessment of the generated images – see Fig. 2. The physical IQ was used to minimise subjective bias in choosing 80 images covering the full range of SNR levels (including the median) out of the full image bank that contained 792 images. Eighty images were shown to a visual focus group of examiners to select the reference image. This was done to ensure in it would have an intermediate level (median) of sharpness and noise. Selecting the reference image in this way was undertaken in order to allow the observer to use the whole of the Likert scale during relative VGA and thus reduce skewness during scoring [28]. A similar approach for choosing reference images was used by Mraity (2015) [29] and supported by Lance et al. (2014) [30].

The lead researcher performed the relative VGA evaluations. This observer had his performance sample-tested against five experienced radiographers (> 5 years post-qualification experience), which is represented by inter class correlation (ICC). The ICC results for the 'sharpness' criteria varied from 0.827 (95% CI 0.731 to 0.889) to a maximum of 0.937 (95% CI 0.886 to 0.963), while the 'noise' criteria showed a minimum ICC value of 0.93 (95% CI 0.874 to 0.959) and a maximum 0.971 (95% CI 0.947 to 0.983). The observed range of ICC, according to Rosner [31] (2010), showed excellent agreement.

Table 1
Exposure factors that scored the five lowest doses with acceptable IQ (10-year-old).

Optimum acquisitions (AEC): 10-year-old							
Dose rank	kVp	SID	Filtration (mm)	Chambers	Or	IAK (μGy)	DAP (mGy cm^2)
1	89	130	1 Al + 0.1 Cu	Both outer	HT	178.77	73
2	89	115	1 Al + 0.1 Cu	Both outer	HT	184.07	74
3	89	130	1 Al + 0.1 Cu	All	HT	187.53	77
4	89	140	1 Al + 0.1 Cu	Both outer	HT	188.57	73
5	89	115	1 Al + 0.1 Cu	All	HT	193.17	78

Or: Orientation

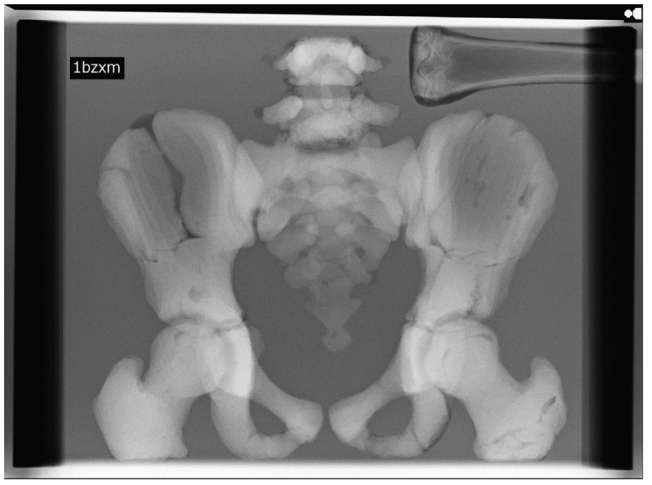

(a)

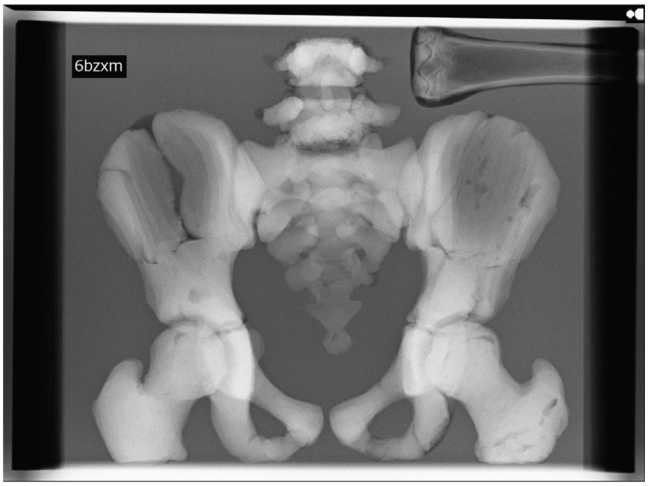

(b)

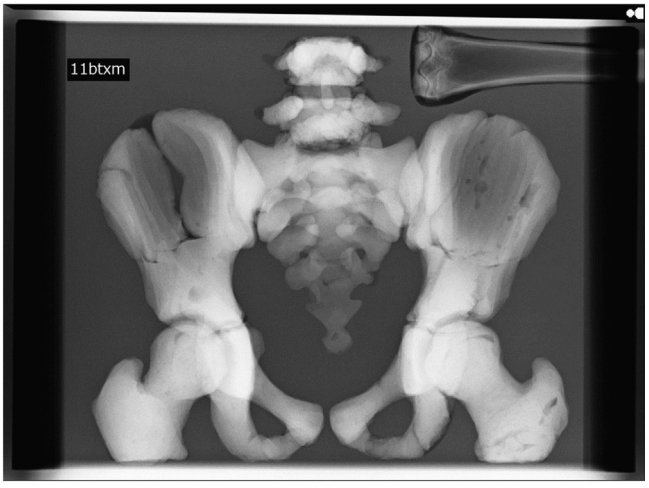

(c)

Fig. 3. (a, b and c): represents images of different IQ levels. (Two outer AEC chambers, HA orientation, zero filtration, and 115 cm SID).

The absolute visual grading assessment involved the use of 84 images, which covered all the IQ levels identified in the relative VGA evaluation. The largest proportion of these represented the intermediate level of IQ. The highest and lowest visual IQ scores had approximately five images each, and the rest were in the middle (intermediate) level. This distribution provided the opportunity to score more images from the levels of IQ with the least consensus. For the 84 images, they were displayed to two consultant radiologists (> 30 years clinical experience each), who provided an independent opinion as to whether each image was of diagnostic quality (by observing the anatomical structures portrayed in the phantom images, which included the animal bone). Their opinions were binary in response (yes or no).

The purpose of combining the two VGA methods was to reduce the number of images displayed to radiologists, as scoring 792 images would take too long.

The relative VGA yields an IQ scale for each image making it possible to analyse trends when changing exposure parameters. Thus, we are able to examine the relative impact of each exposure factor compared to the other factors.

2.3. Data analysis

A data normality check was performed when comparison between groups was needed. Non-parametric tests were performed, depending on the Shapiro-Wilko result (a significant value, $P < 0.05$, indicated a non-parametric distribution) [32]. The Wilcoxon and Friedman tests were considered for comparisons between groups for non-parametric data. Finally, all data analyses were undertaken using SPSS (IBM Inc, Armonk, NY).

2.3.1. Dose optimised techniques

The exposure factor combinations that produced 'acceptable image quality' for the five lowest doses were displayed in a table to present the recommended exposure techniques for the paediatric pelvis imaging of a 10-year-old child. The reason for providing the lowest five doses was to help identify alternative exposure factors should the need arise. The doses for each exposure factor combination were included to aid understanding of the corresponding level of radiation exposure, as well as to compare with dose measurements usually found in clinical practice (such as the DAP). In addition, comparisons were undertaken between the two orientations (HT and HA) and AEC chamber combinations, in terms of dose and image quality.

2.3.2. Regression analysis

The regression test was conducted for IQ and radiation dose, whilst including the exposure factors as dependent variables. This was performed to identify the size of the impact between the different exposure factors and to assess their relationship when combined. The HT orientation was used for the regression analysis as it demonstrated lower radiation dose according to the Wilcoxon signed rank test ($p < 0.05$). Within this orientation, the two outer AEC chambers were also fixed in the regression model, since it yielded the lowest radiation dose according to the Friedman test ($p < 0.05$). This was performed to identify the size / type of the impact yielded the lowest radiation dose according to the Friedman test. The amount and the type of impact from each exposure factor can be identified via determining the regression coefficient (β). The relative impact size was measured by dividing β for each two exposure factors. This technique was performed for IQ and radiation dose. The regression method was chosen with a free (non-zero) intercept. The justification for this is that the AEC compensates by keeping the quantity of radiation reaching the image detector the same, regardless of an increased SID or added filtration. Thus, there is no possibility of assuming the dose to the patient will approach zero if the SID and/or additional filtration are at infinity.

The method for constructing the regression model was the forced method (or Entry Method). This method includes no effect from the order of predictors on the estimation of the regression model [32,33].

3. Results

3.1. Dose optimised technique

Two radiologists evaluated the 84 images and confirmed that all of

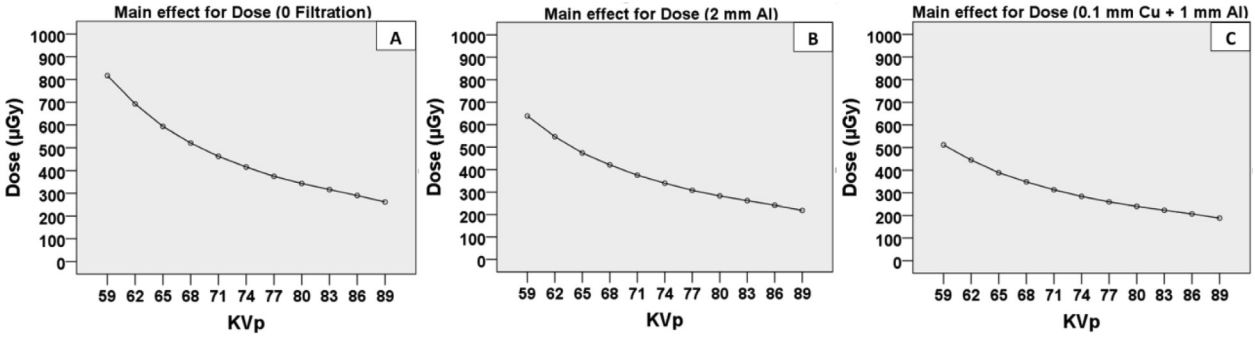

Fig. 4. (A, B and C): 10 year-old the main effect plots for dose (µGy) when increasing the kVp; (A) at 0 filtration, (B) at 2 mm Al, (C) at 0.1 mm Cu + 1 mm Al.

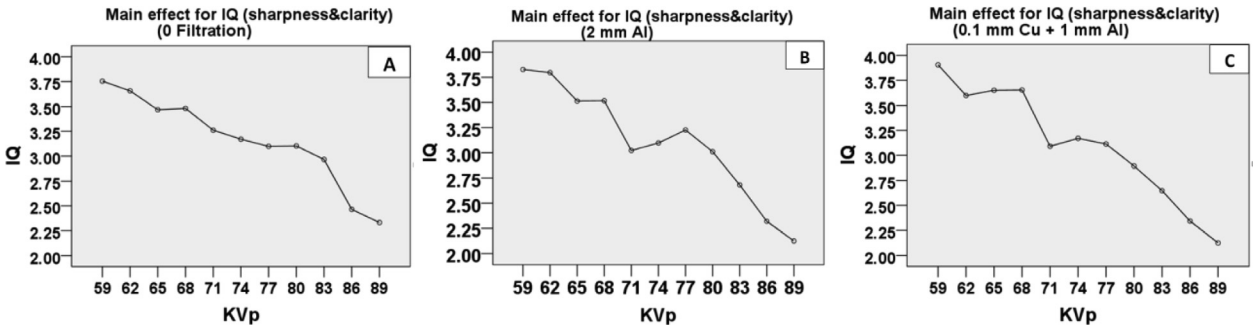

Fig. 5. (A, B and C): 10 year-old the main effect plots for IQ (sharpness and clarity) when increasing the kVp. (A) at 0 filtration, (B) at 2 mm Al and (C) at 0.1 mm Cu + 1 mm Al.

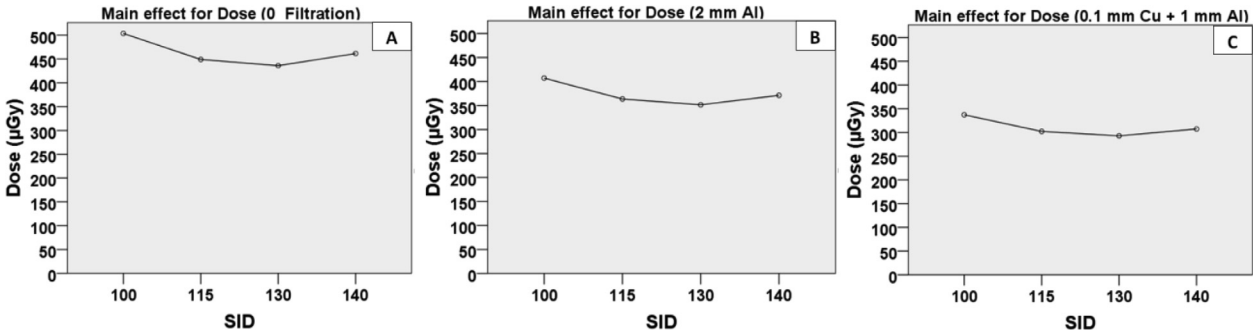

Fig. 6. (A, B and C): 10 year-old the main effect plots for dose (µGy) when increasing the SID; (A) at 0 filtration, (B) at 2 mm Al, (C) at 0.1 mm Cu + 1 mm Al.

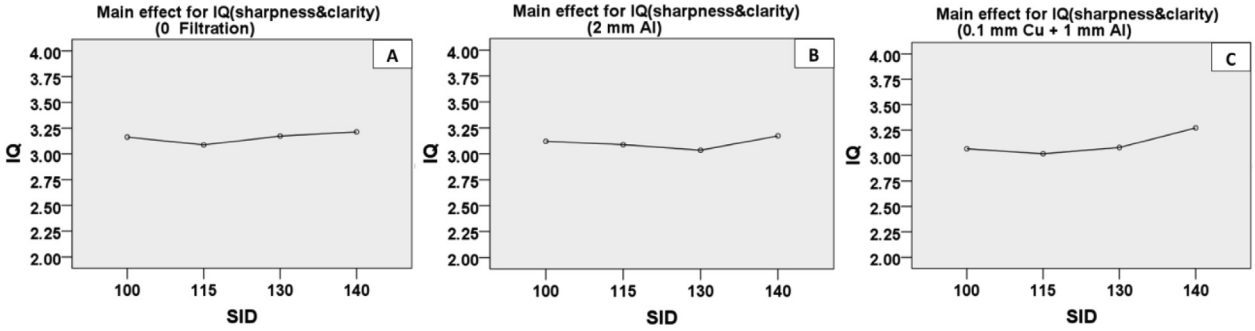

Fig. 7. (A, B and C): 10 year-old the main effect plots for IQ (sharpness and clarity) when increasing the SID. (A) at 0 filtration, (B) at 2 mm Al and (C) at 0.1 Cu + 1 mm Al.

the images were of acceptable IQ for diagnostic purposes. The optimisation study on 792 images showed that the five optimum (lowest dose) exposure factor combinations were all at 89 kVp (Table 1). The lowest exposure technique was with 89 kVp, 130 cm SID, 1 mm Al + 0.1 mm Cu of additional filtration and in the HT orientation with two outer AEC chambers selected – see Table 1. The five lowest radiation doses ranged from 178.77 to 193.17 µGy, and all were with 1 mm Al + 0.1 mm Cu of additional filtration. This means that, despite the variations in IQ levels, all images were of clinically acceptable quality (see Fig. 3). The percentage reduction in radiation dose reached 87.3% within this study (with a range of 178.77 µGy to 1405 µGy). Also within the dose optimised exposure techniques described in Table 1 the dose reduction is

Table 2
Absolute β values (in descending order) for each exposure factor, along with their ratios.

Regression			
Radiation dose		IQ	
Exposure factor	± |β|	Exposure factor	± |β|
Filter	−76.24	kVp	−0.05
kVp	−13.44	Filter	−0.03
SID	−0.96	SID	0.002
Exposure factor |β| ratio			
Radiation dose		IQ	
Filter/kVp	5.67	kVp/Filter	1.99
$\frac{(\text{Filter / kVp})_{Radaitiondose}}{(\text{Filter / kVp})_{IQ}} = 11.28$			
Filter/SID	79.18	Filter/SID	11.30
$\frac{(\text{Filter / SID})_{Radaitiondose}}{(\text{Filter / SID})_{IQ}} = 7.01$			
kVp/SID	13.96	kVp/SID	22.52
$\frac{(\text{kVp / SID})_{Radaitiondose}}{(\text{kVp / SID})_{IQ}} = 0.62$			

Table 3
The full details for the constructed dose and IQ regression models.

Regression (10 year old)					
		Dose		IQ	
	R^2	0.89		0.78	
	P (F-test)	0.001		0.001	
	Constant	1569.41		6.65	
kVp	B|P-value	−13.44	0.001	−0.05	0.001
	95%CI	−14.34		−0.06	
		−12.53		−0.05	
SID	B|P-value	−0.96	0.01	0.002	0.01
	95%CI	−1.53		−0.001	
		−0.40		0.005	
Filtration	B|P-value	−76.24	0.001	−0.03	0.03
	95%CI	−86.76		−0.08	
		−65.72		0.03	

Table 4
Anteroposterior pelvis image quality scale introduced by Mraity et al. (2016).

No	IQ criteria
1	The left hip joint is adequately visualized.
2	The right hip joint is adequately visualized.
3	The right lesser trochanter is visualized adequately.
4	The left lesser trochanter is visualized adequately.
5	The left greater trochanter is visualized adequately.
6	The right greater trochanter is visualized adequately.
7	The left iliac crest is adequately visualized.
8	The right iliac crest is adequately visualized.
9	The pubic and ischial rami are not adequately visualized.
10	The proximal femora are demonstrated adequately.
11	The left femoral neck is visualized adequately.
12	The right femoral neck is visualized adequately.
13	The left sacroiliac joint is visualized adequately.
14	The right sacroiliac joint is visualized adequately.
15	The sacrum and its intervertebral foramina are not visualized adequately.

7.5% (minimum: 178.77 μGy and maximum 193.17 μGy). The optimisation study was undertaken for the two orientations (HT and HA), however the lowest doses were found in the HT orientation. The study also showed that the chamber combinations (two outer and all three chambers) generated the lowest doses (See Figs. 4–7).

Using the Friedman test, no significant difference to diagnostic IQ was found when changing the SID (100–140 cm), however there was a significant effect on radiation dose for both orientations with all AEC chamber combinations. The two-outer chamber combination produced the lowest dose when compared with the other AEC chambers combinations, and differences were statistically significant (Friedman test).

3.2. Regression

The regression analysis showed that the R squared value ranged from 0.86 to 0.99. The study showed that all β values were statistically significant ($p < 0.05$).

The regression models for radiation dose showed that the first, second and third highest impacting variables were filtration, kVp and SID, respectively. The first, second and the third highest impacting variables on IQ were kVp, filtration and SID, respectively. All the exposure factors showed a negative impact on IQ and radiation dose, except for the effect of SID on IQ (Table 2).

Regarding the β ratios between exposure factors, the dose regression model showed that the largest impact ratio was filtration to SID (79.2), and the second largest was kVp to SID (13.96), respectively. Filtration to kVp had the lowest impact ratio (5.7) (Table 2). The regression model for IQ showed that the largest impact ratio on this IQ scale was kVp to SID (22.5), and that the second largest impact ratio was filtration to SID (11.3). The kVp showed approximately twice the impact of filtration on IQ, where their ratio was 2.0 (Table 2). Table 3 contains the full details for the dose and IQ regression models.

4. Discussion

4.1. Dose optimised technique

The results in Table 1 suggest that using a high tube potential (89 kVp) would promote dose optimised imaging, as seen in the results which used dose optimised exposure factors, which had the highest kVp considered in our study. This agrees with the literature wherein using a high kVp is supported as a dose reduction technique [34].

SID had a significant effect on radiation dose, and a non-significant effect on diagnostic IQ. This could be related to the low sensitivity of human perception to subtle differences which can be generated by the continuous compensation of the AEC chambers [35]. Within the factorial experiment, the reduction in the radiation dose range was from 1405 μGy to 178.77 μGy. This resulted in an 87.3% reduction in dose (dose difference: 1226.23 μGy), whilst maintaining acceptable image quality. This reduction is related to the effect of increasing the X-ray beam energy (kVp), SID and possibly the AEC chambers not fully compensating for the reduction in radiation dose [29]. Our results agree with findings in the literature for AEC imaging studies, but these used adult pelvis phantoms [36,37].

All of the diagnostically acceptable images, with the five lowest doses (Table 1), were with 1 mm Al + 0.1 mm Cu additional filtration. This can be explained by the ability of filtration to remove the low energy X-ray photons and, hence, reduce radiation doses [21]. Also, results using the Friedman test demonstrate that the added filtration had a significant effect (reduction) on radiation dose, with no significant effect on diagnostic IQ. This was observed for the HT orientation for all AEC chamber combinations. The significant effect of reduction in "patient" dose can be reasoned by the beam hardening that causes a reduction in the dose. The non-significant effect of added filtration on IQ can also be related to beam hardening. This can reduce IQ while the radiation dose is compensated by the AEC mode. The effect of increasing the average energy of the beam on IQ is reduced by the wide dynamic range of the digital imaging system which maintains image contrast [38].

4.2. Discussion for β

Amongst all the exposure factors investigated, the SID showed the lowest impact on radiation dose (−β) and on diagnostic IQ (+β) in the

regression models (Table 2). The lowest impact of SID on radiation dose and IQ can be justified by the compensation of the ionisation chambers during the AEC imaging mode. Filtration and kVp have a higher impact as they both increase the average energy of the X-ray beam. In addition to changing the amount of radiation, the AEC does not prevent the effect on radiation dose and IQ of the changes in the X-ray energy. Additional filtration showed the highest impact on reducing radiation dose ($-\beta$), while also showing the second highest impact after kVp on diagnostic IQ ($-\beta$). The comparison between filtration and kVp effect's on IQ can be explained by the level at which image contrast is decreased, wherein kVp can increase average X-ray energy more than filtration.

On the other hand, the ratios between β of each exposure factor leads to other conclusions. The kVp to SID impact proportions in the regression model were approximately 14 for radiation dose and 22.5 for diagnostic IQ (Table 2). This means that the effect of changing both kVp and SID was about the same (their ratios are about 0.62 times for both kVp and SID) on radiation dose and diagnostic IQ. However, SID showed a positive impact on diagnostic IQ and a negative impact on radiation dose. Thus, the results suggest increasing SID as a preferred choice for dose reduction. For 'additional filtration' to 'SID manipulation', the impact ratio on radiation dose (79.2) was larger than on diagnostic IQ (11.3) by about seven times. This means that the effect of changing filtration (compared to SID) is approximately seven times more for radiation dose than for diagnostic IQ. This makes filtration the preferred option when compared to SID. However, the SID showed a positive impact on diagnostic IQ (Table 2). Thus, the results suggest using a larger SID and higher filtration levels.

The impact ratio of filtration to kVp on radiation dose (5.67) was greater than that of diagnostic IQ (1/1.99), by about eleven times (11.28). This means that increasing filtration (compared to kVp) has eleven times greater of an effect on radiation dose than it does on diagnostic IQ. Thus, the results recommend using higher filtration rather than increasing kVp. This agrees with the literature, wherein it is suggested that 1 mm Al with 0.1 to 0.2 mm Cu be used for paediatric and adult imaging [39]. Comparison with literature is limited due to the AEC imaging mode which compensates for the reduced radiation when adding additional filtration, unlike in the manual mode. Thus, the effect of filtration for AEC imaging is different when compared to manual imaging, which makes comparisons problematic.

4.3. Limitations

There is a limited number of simulated tissues in the pelvis phantom, including the soft tissue and cortical bones. Tissues like the trabecular bone and other soft tissues (bladder, testis or ovary) were not included. However, the tissues included within the pelvis phantom are those which are typically represented on paediatric AP pelvis X-ray images to visualise the edges of bone structures. They are also considered to be a key imaging priority [40,41]. Since the phantom under investigation lacks pathology, our optimisation results are limited to normal cases only. Also, there is the possibility of carrying out additional optimisation by changing the adjustment of the sensitivity of the AEC, as they were kept to the manufacturer's default settings within our work. One more point to highlight is that this study considered 89 as the highest value for kVp. Further work could explore using higher kVp values.

5. Conclusion

Factorial experimental design studies were undertaken to provide a systematic optimisation of the radiation doses used in clinical digital paediatric AP pelvis radiography for 10-year olds. Exposure factor combinations were identified according to their ability to produce diagnostically acceptable X-ray images with the lowest radiation dose. Also, there is a unified conclusion that the use of additional filtration (1 mm Al + 0.1 mm Cu) universally reduces dose while maintaining IQ.

The regression analysis demonstrated the impact of each exposure factor in terms of its effect size and relative effect size on IQ and radiation dose. This helped us to understand which exposure factors and techniques can be used beneficially to reduce paediatric doses. The regression also highlighted two points – firstly, it demonstrated that increasing the SID would be advantageous, as it reduces the radiation dose with no significant effect on diagnostic IQ, and secondly, that increasing the filtration level is more a priority than increasing the kVp.

Declaration of Competing Interest

The authors declare that they have no known competing financial interests or personal relationships that could have appeared to influence the work reported in this paper.

References

[1] Vaño E, Fernández JM, Ten JI, Prieto C, González L, Rodríguez R, et al. Transition from screen-film to digital radiography: evolution of patient radiation doses at projection radiography. Radiology 2007;243:461–6. https://doi.org/10.1148/radiol.2432050930.
[2] Al Khalifah K, Brindhaban A. Comparison between conventional radiography and digital radiography for various kVp and mAs settings using a pelvic phantom. Radiography 2004;10:119–25. https://doi.org/10.1016/j.radi.2004.02.006.
[3] Mc Fadden S, Roding T, de Vries G, Benwell M, Bijwaard H, Scheurleer J. Digital imaging and radiographic practise in diagnostic radiography: an overview of current knowledge and practice in Europe. Radiography 2017:8–12. https://doi.org/10.1016/j.radi.2017.11.004.
[4] Martin L, Ruddlesden R, Makepeace C, Robinson L, Mistry T, Starritt H. Paediatric x-ray radiation dose reduction and image quality analysis. J Radiol Prot 2013;33:621–33. https://doi.org/10.1088/0952-4746/33/3/621.
[5] Paulo G, Santos J, Moreira A, Figueiredo F. Transition from screen-film to computed radiography in a paediatric hospital: the missing link towards optimisation. Radiat Prot Dosim 2011;147:164–7. https://doi.org/10.1093/rpd/ncr355.
[6] Almen A, Mattsson S. The radiation dose to children from X-ray examinations of the pelvis and the urinary tract. Br J Radiol 1995;68:604–13. https://doi.org/10.1259/0007-1285-68-810-604.
[7] Precht H, Gerke O, Rosendahl K, Tingberg A, Waaler D. Large dose reduction by optimization of multifrequency processing software in digital radiography at follow-up examinations of the pediatric femur. Pediatr Radiol 2014;44:239–40. https://doi.org/10.1007/s00247-013-2854-3.
[8] Brosi P, Stuessi A, Verdun F, Vock P, Wolf R. Copper filtration in pediatric digital X-ray imaging: Its impact on image quality and dose. Radiol Phys Technol 2011;4:148–55. https://doi.org/10.1007/s12194-011-0115-4.
[9] Almen A, Lööf M, Mattsson S. Examination technique, image quality, and patient dose in paediatric radiology. Acta Radiol 1996;37:337–42. https://doi.org/10.1177/02841851960371P171.
[10] Veldkamp WJH, Kroft LJM, Boot MV, Mertens BJA, Geleijns J. Contrast-detail evaluation and dose assessment of eight digital chest radiography systems in clinical practice. Eur Radiol 2006;16:333–41. https://doi.org/10.1007/s00330-005-2887-6.
[11] Bloomfield C, Boavida F, Chabloz D, Crausaz E, Huizinga E, Hustveite H, et al. Experimental article – reducing effective dose to a paediatric phantom by using different combinations of kVp, mAs and additional filtration whilst maintaining image quality. Lisbon, Portugal: OPTIMAX 2014 – radiation dose and image quality optimisation in medical imaging; 2015.
[12] McEntee M, Doherty P. Optimisation of the pediatric pelvis radiographic examination. ECR 2011 (Poster No C-0265) 2011:1–7. doi:10.1594/ecr2011/C-0265.
[13] Butler M-L, Brennan P. Nonselective Filters Offer Important Dose-Reducing Potential in Radiological Examination of the Paediatric Pelvis. J Med Imaging Radiat Sci 2009;40:15–23. https://doi.org/10.1016/j.jmir.2008.11.002.
[14] CIRS Tissue Simulation and Phantom Technology. ATOM ® Dosimetry Phantoms: Models 701-706 2011:16.
[15] Norrman E, Persliden J. A factorial experiment on image quality and radiation dose. Radiat Prot Dosim 2005;114:246–52. https://doi.org/10.1093/rpd/nch557.
[16] Montgomery D. Design and analysis of experiments. 8th ed. John Wiley & Sons, Inc.; 2013.
[17] Andria G, Attivissimo F, Guglielmi G, Lanzolla AML, Maiorana A, Mangiantini M. Towards patient dose optimization in digital radiography. Measurement 2016;79:331–8. https://doi.org/10.1016/j.measurement.2015.08.015.
[18] Uffmann M, Schaefer-Prokop C. Digital radiography: The balance between image quality and required radiation dose. Eur J Radiol 2009;72:202–8. https://doi.org/10.1016/j.ejrad.2009.05.060.
[19] Martin CJ. Optimisation in general radiography. Biomed Imaging Interv J 2007;3.. https://doi.org/10.2349/biij.3.2.e18.
[20] CEC. European Guidelines on quality criteria for diagnostic radiographic images in paediatrics; 1996.
[21] Fauber T. Radiographic imaging and exposure. 4th ed. Elsevier Health Sciences; 2013.

[22] Mohammed Ali A, Hogg P, Johansen S, England A. Construction and validation of a low cost paediatric pelvis phantom. Eur J Radiol 2018;108:84–91. https://doi.org/10.1016/j.ejrad.2018.09.015.
[23] Institute of Physics and Engineering in Medicine (IPEM). IPEM report 91 recommended standards for the routine performance testing of diagnostic X-ray imaging systems. York; 2005.
[24] Båth M. Evaluating imaging systems: practical applications. Radiat Prot Dosim 2010;139:26–36. https://doi.org/10.1093/rpd/ncq007.
[25] Hogg P, Blindell P. Software for image quality evaluation using a forced choice method. Manchster, UK: Pap Present UKRC; 2012.
[26] Norweck J, Seibert J, Andriole K, Clunie D, Curran B, Flynn M, et al. ACR–AAPM–SIIM technical standard for electronic practice of medical imaging. J Digit Imaging 2013;26:38–52. https://doi.org/10.1007/s10278-012-9522-2.
[27] Mraity H, England A, Cassidy S, Eachus P, Dominguez A, Hogg P. Development and validation of a visual grading scale for assessing image quality of AP pelvis radiographic images. Br J Radiol 2016;89:20150430. https://doi.org/10.1259/bjr.20150430.
[28] Allen E, Hogg P, Ma W, Szczepura K. Fact or fiction: an analysis of the 10 kVp 'rule' in computed radiography. Radiography 2013;19:223–7. https://doi.org/10.1016/j.radi.2013.05.003.
[29] Mraity H. Optimisation of radiation dose and image quality for AP pelvis radiographic examination. University of Salford; 2015.
[30] Lança L, Franco L, Ahmed A, Harderwijk M, Marti C, Nasir S, et al. 10kVp rule – an anthropomorphic pelvis phantom imaging study using a CR system: Impact on image quality and effective dose using AEC and manual mode. Radiography 2014;20:333–8. https://doi.org/10.1016/j.radi.2014.04.007.
[31] Rosner B. Fundamentals of biostatistics. 7th ed. Cengage Learning, Inc; 2010.
[32] Field A. Discovering statistics using IBM SPSS statistics. 4th ed. London: Sage Publications Ltd.; 2013.
[33] Field A, Miles J, Field Z. Discovering statistics using R. Sage Publications Ltd.; 2012.
[34] Herrmann T, Fauber TL, Gill J, Hoffman C, Orth DK, Peterson P a, et al. Best practices in digital radiography. Radiol Technol 2012;84:83–9. doi:84/1/83 [pii].
[35] Smith NB, Webb A. Introduction to medical imaging: physics, engineering and clinical applications. Cambridge University Press; 2010.
[36] Brennan P, McDonnell S, O'Leary D. Increasing film-focus distance (FFD) reduces radiation dose for x-ray examinations. Radiat Prot Dosim 2004. https://doi.org/10.1093/rpd/nch029.
[37] Tugwell J, Everton C, Kingma A, Oomkens DM, Pereira GA, Pimentinha DB, et al. Increasing source to image distance for AP pelvis imaging – impact on radiation dose and image quality. Radiography 2014;20:351–5. https://doi.org/10.1016/j.radi.2014.05.012.
[38] Hansson J, Båth M, Håkansson M, Grundin H, Bjurklint E, Orvestad P, et al. An optimisation strategy in a digital environment applied to neonatal chest imaging. Radiat Prot Dosim 2005;114:278–85. https://doi.org/10.1093/rpd/nch528.
[39] Alzen G, Benz-Bohm G. Radiation protection in pediatric radiology. Dtsch Aerzteblatt Online 2011;108:407–14. https://doi.org/10.3238/arztebl.2011.0407.
[40] Singh M, Riggs BL, Beabout JW, Jowsey J. Femoral trabecular-pattern index for evaluation of spinal osteoporosis. Ann Intern Med 1972;77:63–7. https://doi.org/10.7326/0003-4819-77-1-63.
[41] Stieve FE. Radiological requirements for the specification of image quality criteria. Optim Image Qual Patient Expo Diagnostic Radiol BIR Report 1989;20:221–38.